Nicotinamidase participates in the salvage pathway of NAD biosynthesis in Arabidopsis

Guodong Wang and Eran Pichersky[*]

Department of Molecular, Cellular and Developmental Biology, University of Michigan, 830 North University Street, Ann Arbor, MI 48109-1048, USA

Summary

Nicotinamide adenine dinucleotide (NAD) and nicotinamide adenine dinucleotide phosphate (NADP), which is derived from NAD, have important roles as a redox carriers in metabolism. A combination of *de novo* and salvage pathways contribute to the biosynthesis of NAD in all organisms. The pathways and enzymes of the NAD salvage pathway in yeast and animals, which diverge at nicotinamide, have been extensively studied. Yeast cells convert nicotinamide to nicotinic acid, while mammals lack the enzyme nicotinamidase and instead convert nicotinamide to nicotinamide mononucleotide. Here we show that *Arabidopsis thaliana* gene *At2g22570* encodes a nicotinamidase, which is expressed in all tissues, with the highest levels observed in roots and stems. The 244-residue protein, designated AtNIC1, converts nicotinamide to nicotinic acid and has a K_m value of 118 ± 17 μM and a K_{cat} value of 0.93 ± 0.13 sec^{-1}. Plants homozygous for a null AtNIC1 allele, *nic1-1*, have lower levels of NAD and NADP under normal growth conditions, indicating that AtNIC1 participates in a yeast-type NAD salvage pathway. Mutant plants also exhibit hypersensitivity to treatments of abscisic acid and NaCl, which is correlated with their inability to increase the cellular levels of NAD(H) under these growth conditions, as occurs in wild-type plants. We also show that the growth of the roots of wild-type but not *nic1-1* mutant plants is inhibited and distorted by nicotinamide.

Keywords: Nicotinamide, nicotinic acid, nicotinamidase, stress treatment, abscisic acid.

Introduction

β–Nicotinamide adenine dinucleotide (NAD) and β-nicotinamide adenine dinucleotide phosphate (NADP) are essential compounds in all organisms, serving as coenzymes which are interconverted between the oxidized and reduced forms in redox reactions. All organisms synthesize NAD(P) via a *de novo* pathway from tryptophan and/or aspartate (Figure 1; Katoh and Hashimoto, 2004; Katoh *et al.*, 2006; Rongvaux *et al.*, 2003).

In yeast and animals, catabolism of NAD may involve the release of nicotinamide (NIM) by the enzyme NAD glycohydrolases (Hekimi and Guarente, 2003; Lin *et al.*, 2000). This reaction has not yet been reported in plants. Free NIM can be salvaged and used in the synthesis of NAD in at least two ways (Figure 1). In bacteria and yeast, the Preiss–Handler pathway involves the hydrolysis of NIM by nicotinamidase (NIC; EC 3.5.1.19) to nicotinic acid (NA), then the synthesis of nicotinic acid mononucleotide (NaMN) by the enzyme nicotinic acid phosphoribosyl transferase (NaPR-

Tase). Nicotinic acid mononucleotide is then fed into the *de novo* pathway (Figure 1). In mammals, which appear to lack NIC, NIM is directly converted to nicotinamide mononucleotide (NMN) by nicotinamide phosphoribosyltransferase (NRPTase; Schweiger *et al.*, 2001), then to NAD by nicotinamide mononucleotide adenylyltransferase (NMNAT; Raffaelli *et al.*, 2002; Zhang *et al.*, 2003). Recently, Bieganowski and Brenner (2004) reported that fungi and mammals can take up exogenously added nicotinamide riboside and phosphorylate it using nicotinamide riboside kinase (Nrk1) to form NMN, which is then converted to NAD as in mammalian cells (Figure 1).

In the NAD *de novo* pathway, NAD kinase (NADK) catalyzes NADP$^+$ formation by using NAD$^+$ and ATP as substrates (NADK cannot use NADH as a substrate; Kawai *et al.*, 2001). While NADPH can be generated from NADP$^+$ through the electron-transfer reactions of photosynthesis, in non-photosynthetic tissues NADPH is generated from

Figure 1. *De novo* and salvage pathways of NAD biosynthetic pathways.
The reactions marked with black arrows constitute the *de novo* pathway. While the start of the pathway varies among organisms, some of which use Trp and others Asp (Arabidopsis uses Asp, see Katoh *et al.*, 2006), the same two reactions from NaMN to NAD(H) apparently occur in all organisms. The salvage reaction marked with a purple arrow has been reported from bacteria, yeast and animals, but not yet from plants. The salvage reactions marked with blue arrows have been reported from fungi and bacteria, and the reactions marked in red arrows have been reported from mammals. Reactions that have been inferred to occur in plants, based on results from labeling experiments, are shown with dotted green arrows. NaAD, nicotinate adenine dinucleotide; NaMN, nicotinate mononucleotide; NMN, nicotinamide mononucleotide; NaMNAT, nicotinate mononucleotide adenylyl transferase; NaPRTase, nicotinate phosphoribosyltransferase; NIC, nicotinamidase (named in yeast as PNC1); NMNAT, nicotinamide mononucleotide adenylyl transferase; NPRTase, nicotinamide phosphoribosyltransferase; Nrk1, nicotinamide riboside kinase1.
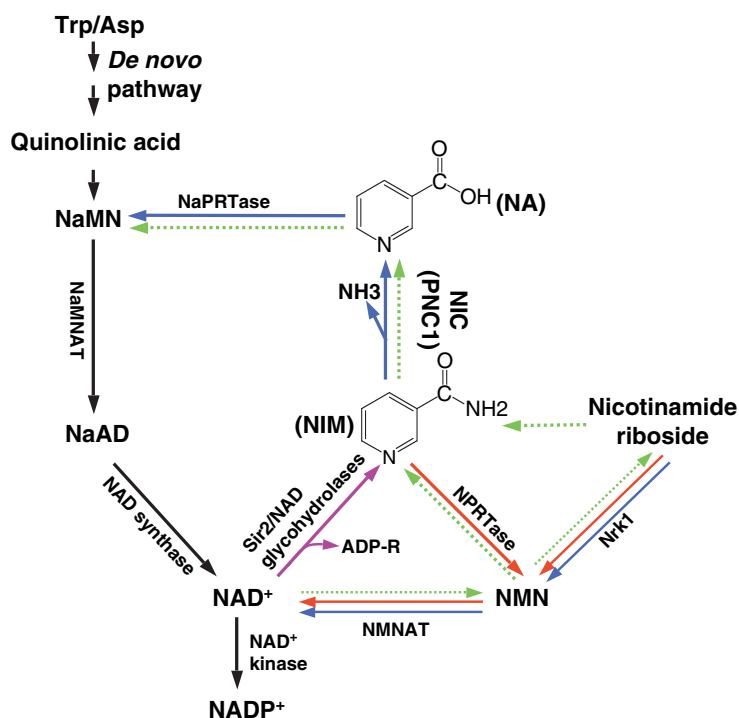
$NADP^+$ primarily by glucose-6-phosphate dehydrogenase and 6-phosphogluconate dehydrogenase through the pentose phosphate pathway (Corpas *et al.*, 1998). In addition, an NADH kinase that contains a NADK-like domain and preferentially uses NADH rather than NAD^+ as a substrate has been identified in yeast (Outten and Culotta, 2003) and Arabidopsis (Turner *et al.*, 2005).

The first step in the Preiss–Handler salvage pathway of NIM requires the activity of NIC. This enzyme was first reported by Hughes and Williamson (1953), and has since been described in various microorganisms and in plants (Zheng *et al.*, 2005), but not in mammals (Hunt *et al.*, 2004; Katoh and Hashimoto, 2004). A gene encoding yeast NIC has been reported by Ghislain *et al.* (2002) and designated *PNC1* (*Pyridine Nucleotide Cycle1*). A search of the Arabidopsis genome using the yeast *PNC1* sequence identified several homologs (Hunt *et al.*, 2004; Katoh and Hashimoto, 2004; Rongvaux *et al.*, 2003).

Although the *de novo* and the alternative salvage pathways to NAD have been studied in some detail in animals and microorganisms, much less is known about these pathways in plants. Nonetheless, tracer experiments (Ashihara *et al.*, 2005; Zheng and Ashihara, 2004; Zheng *et al.*, 2005) and enzymatic assays (Wagner and Wagner, 1985; Wagner *et al.*, 1986) have examined specific steps in both the *de novo* pathway and the salvage pathway in plants. Zheng *et al.*, in their studies of the biosynthesis of pyridine alkaloids in *Coffea arabica* and *Phaseolus aureus*, showed that both NIM and NA could be incorporated into NAD when fed to plant tissues (Zheng and Ashihara, 2004;

Zheng *et al.*, 2005). They further noted that in preliminary experiments they could not identify NPRTase activity but did detect some NIC activity (Zheng *et al.*, 2005). Labeling studies in plants also suggested that there are two additional paths from NAD to NIM besides the reaction catalyzed by Sir2/NAD glycohydrolase: in one, NAD is converted to NMN, then to NIM (Zheng and Ashihara, 2004), and in another pathway NAD is converted to NMN and then to nicotinamide riboside, which can then be converted to NIM (Ashihara *et al.*, 2005; Zheng *et al.*, 2005).

In addition to its role in the NAD salvage pathway, NIM has been implicated in several other processes in plants. For example, it has been hypothesized to function as an initial signal in the defensive response to DNA-strand breakage caused by oxidative stress and/or by specific chemicals (Berglund *et al.*, 1996).

Here, we show that in *Arabidopsis thaliana* gene *At2g22570* encodes a nicotinamidase involved in the NAD salvage pathway. We further show that Arabidopsis plants carrying a mutation in this gene contain lower levels of NAD and NADP and display abnormal hypersensitivity to exogenously added ABA and NaCl.

Results

Arabidopsis plants can convert exogeneously added NIM to NA which is incorporated into NAD(P)

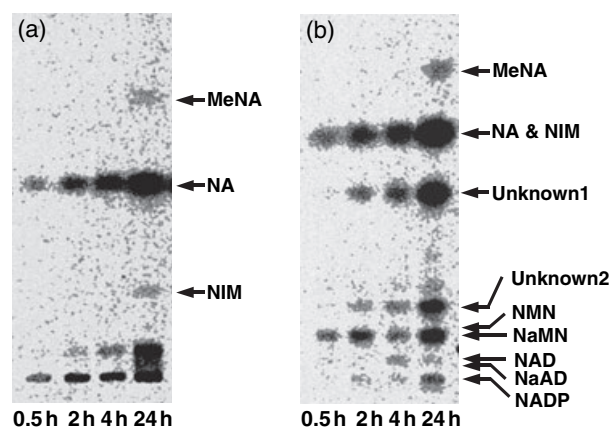To examine whether any NAD salvage pathway operates in Arabidopsis, we treated the leaf disc of Col-0 with 10 μM

Figure 2. Time course studies of the metabolism of exogenously added [^{14}C]-NIM to Arabidopsis leaf discs.
Panels (a) and (b) show the same experiment, but the TLC system shown in (a; EtOAc:HOAc at a 100:1 ratio) separates NA from NIM, while the TLC system employed in (b; *n*-butanol:HOAc:H$_2$O at a 2:1:1 ratio) separates the unresolved bands seen at the bottom of panel (a) but does not separate NA from NIM. Arrows indicate the position of standards.

[^{14}C]-NIM. After 30 min of incubation, almost all the [^{14}C]-NIM that was picked up by the leaf disks was converted to NA, and some was further converted to NaMN (Figure 2). In the course of 24 h, more NA and NaMN are produced from the labeled NIM, and some label is found in NAD and NADP as well as in methylated NA (MeNA) and two unknown compounds. No label was observed in NMN, nor any accumulation of labeled NaAD (Figure 2). These results suggest that Arabidopsis utilizes the same NAD salvage pathway as bacteria and yeast.

Arabidopsis gene At2g22570 encodes NIC1

The labeling results showing the conversion of NIM to NA indicate that Arabidopsis possesses NIC activity in the leaf. A BLAST search for Arabidopsis genes with homology to yeast *NIC* (*PNC1*) identified four genes – *At5g23220*, *At5g23230*, *At3g16190* and *At2g22570* – with low sequence identity to *PNC1*, ranging from 14.6% to 17.8% (Table 1). These genes are annotated as 'isochorismatases/hydrolases'. When we expressed a full-length cDNA of *At2g22570*, encoding a protein of 244 amino acids with no predicted subcellular localization signals (http://www.cbs.dtu.dk/services/TargetP

Table 1 Levels of protein sequence identities among PNC1 from yeast and four Arabidopsis homologs

	PNC1	At2g22570	At3g16190	At5g23220
At2g22570	14.6			
At3g16190	17.8	13.9		
At5g23220	15.6	26.9	35.2	
At5g23230	15.0	13.1	22.5	86.4

Values are expressed as percentage (%).

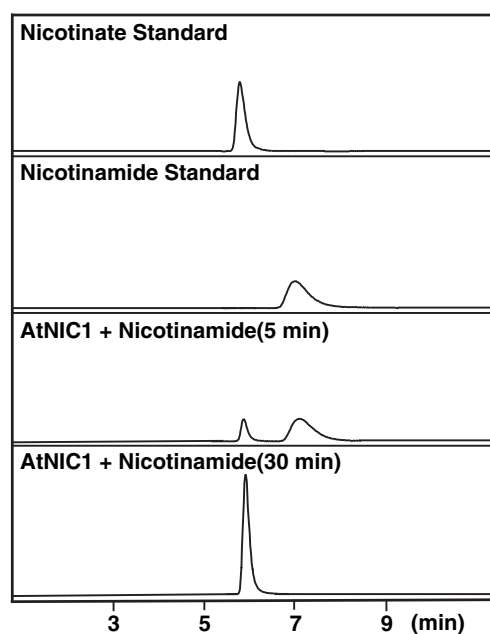**Figure 3.** Time-course analysis of products of the reaction catalyzed by AtNIC1.
Enzyme assays contained 1 mM NIM and 1 μg purified AtNIC1, and were incubated for either 5 min or 30 min, after which reaction products were separated by HPLC as described in Experimental procedures.

/), in *Escherichia coli*, the resulting protein showed NIC activity in enzymatic assays with NIM (Figure 3). [To date, we have not been able to demonstrate NIC activity for the protein encoded by *At3g16190*. Recently, NIC activity was demonstrated for the proteins encoded by *At5g23220* and *At5g23230*, with *At5g23230* being expressed predominantly in the developing embryo (J. E. Gray, University of Sheffield, Sheffield, UK, personal communication).]

Detailed characterization of the protein encoded by *At2g22570* showed that the enzyme was active at the pH range 6–8.5, with optimal activity at pH 6.5–7.0. Nicotinamidase activity was strongly inhibited by 5 mM Zn^{2+}, Cu^{2+}, Fe^{2+} and Fe^{3+} (81–100% inhibition), and was not inhibited at all by Na$^+$, K$^+$ and Ca^{2+} at 5 mM. Mn^{2+} and Mg^{2+} were found to stimulate NIC activity by a factor of 1.3 and 1.7 respectively. An apparent K_m value of 118 ± 17 μM ($n = 3$) for NIM was calculated and the K_{cat} value was 0.93 ± 0.13 sec^{-1} ($n = 3$). The enzyme was also active with pyrazine carboxamide (98% activity when compared with the rate obtained with NIM) and 6-methyl nicotinamide (74%). It did not show any activity with glutamine and 1-methyl nicotinamide. Based on these results, we named the protein encoded by *At2g22570* as AtNIC1.

Expression of AtNIC1 in different tissues

Ribonucleic acid gel blot experiments showed *AtNIC1* transcripts in all organs examined (Figure 4a). The highest levels
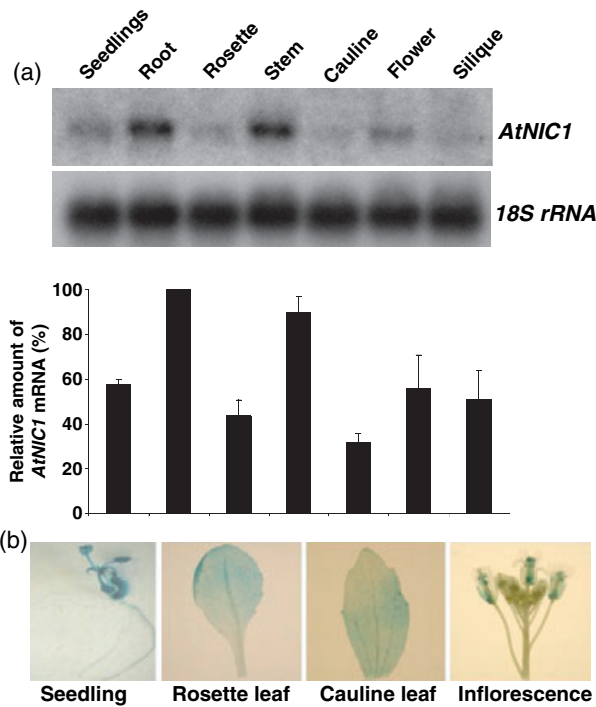
Figure 4. Expression of *AtNIC1* in Arabidopsis.
(a) Ribonucleic acid gel blot analysis of *AtNIC1* transcript levels in different tissues. Ten micrograms of total RNA was loaded in each lane. Top, a representative gel blot of RNA samples from different tissues of wild-type plants. After hybridization with an *AtNIC1* probe, the blot was stripped and rehybridized with an *18S rRNA* probe to control for variation in loading. Bottom, a graphical representation of the results representing the average of three independent experiments.
(b) Histochemical GUS staining of *Pro_{AtNIC1}*:GUS transgenic plants.

of *AtNIC1* transcripts were observed in root and stem, lower levels in flowers and siliques and even lower levels in both rosette and cauline leaves.

The *AtNIC1* expression profile was also examined in plants expressing the *Pro_{AtNIC1}*:GUS transgene. Among eight independent transgenic plants tested, five lines showed GUS activity. In general agreement with RNA blot analysis, the GUS reporter gene under control of the *AtNIC1* promoter was expressed in all tested organs of 10-day-old Arabidopsis seedlings and in most parts of the mature plant, with the exception of the stem (Figure 4b), perhaps because the 1.9-kb promoter fragment used in this experiment (from 1974 to 4 bp upstream the translation initiation codon) does not contain all the elements necessary for the complete function of the *AtNIC1* promoter.

NIC1 enzymatic activity in different organs of Arabidopsis wild-type (Col-0), nic1-1 and AtNIC1-overexpressing plants

Nicotinamidase specific activity was examined in different organs of wild-type plants. Crude protein extracts were made from each organ and incubated with [14C]-NIM; the highest levels of activity were found in root (Figure 5). Nicotinamidase specific activity in stem was 64.7% of the levels seen in root, while levels of NIC specific activity in rosette and cauline leaves, flowers and siliques were three- to fivefold lower than in root. The levels of NIC specific activity in the different organs show a general positive correlation with the levels of *AtNIC1* transcripts in these organs (Figure 4).

We identified one T-DNA insertion line (Col-0 background) in *AtNIC1* from the T-DNA Express database of the Salk

Figure 5. Comparisons of the relative levels of NIC-specific activity in different tissues of Col-0, *nic1-1* and *nic1-1* plants expressing *AtNIC1* under the control of the 35S promoter.
Assays containing [14C]-NIM and 1 μg crude protein extract from the respective organs were incubated at room temperature for 30 min. Reaction products were extracted and run on TLC (top). The quantification of [14C]-NA produced in each reaction is shown below. The complemented lines marked with asterisks were used in further experiments. Data are presented as mean ± SD (n = 5).
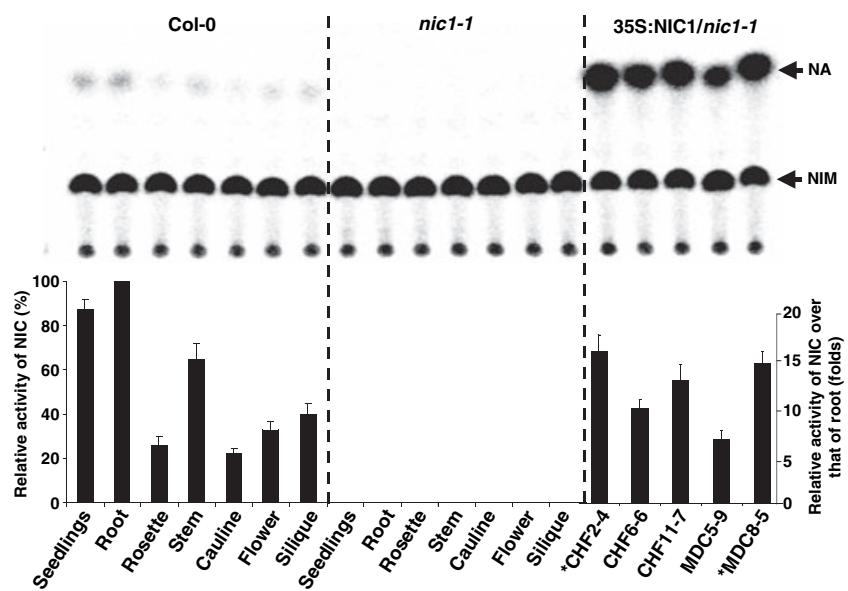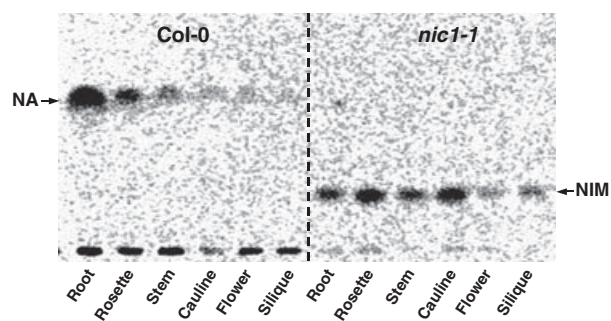
Figure 6. Metabolism of exogenously added [^{14}C]-NIM to intact organs of wild-type and *nic1-1* homozygous plants.
Organs were harvested from 8-week-old plants and immersed in a solution containing 10 μM [^{14}C]-NIM for 4 h. The radiolabeled metabolites were extracted and separated by a TLC plate (EtOAc:HOAc at a 100:1 ratio). Arrows indicate the position of standards.

Institute (http://signal.salk.edu/cgi-bin/tdnaexpress; Alonso *et al.*, 2003) and verified that the insertion occurs in the first exon of the gene at position 117 bp downstream from the start codon. This mutant was designated *nic1-1*. Crude protein extracts from any of the organs of *nic1-1* tested did not show any NIC activity (Figure 5). We also treated the intact organs of *nic1-1* with 10 μM [^{14}C]-NIM, and no other radiolabeled compounds could be detected except for [^{14}C]-NIM itself (Figure 6).

To verify that the lack of NIC activity in the *nic1-1* mutant was due to the insertion in the *AtNIC1* gene, we obtained transgenic plants which express the *AtNIC1* gene under the control of the 35S promoter in the *nic1-1* background (two different binary vectors, CHF3GW and MDC32GW; see Experimental procedures for details). Eighteen independent transgenic plants were confirmed by Northern blot to express the transgenic gene (data not shown), and five lines with the highest *AtNIC1* expression levels were selected for testing NIC activity. These five *35S:NIC1/nic1-1* plants possessed seven- 16-fold higher NIC activity than that found in seedlings of Col-0 (Figure 5).

Levels of NAD(H) and NADP(H) in Col-0, nic1-1 and NIC1-overexpressing plants

Since the NAD salvage pathway through NA appeared to be blocked in the *nic1-1* mutant, we measured and compared the content of NAD(H) and NADP(H) in different organs of wild-type and *nic1-1* mutant plants. The total amounts of NAD(H) and NADP(H) were reduced, from 29% to 67%, in different organs of *nic1-1* mutant plants compared with the corresponding levels in the organs of the wild type at the same growth stage (Table 2). In addition, measurements showed that root and rosette leaves of NIC1-overexpressing transgenic plants had NAD$^+$ and NADH levels that were up to twofold higher than those found in the wild type, but little difference was observed in the concentrations of NADP$^+$ or

NADPH and no significant difference was seen in either the NAD$^+$/NADH or the NADP$^+$/NADPH ratios (Table 2). These data show that the *nic1-1* allele has some effect on NAD biosynthesis but not on the redox state of the cell.

Effects of NIM and NA on root growth

In wild-type seedlings growing on half-strength MS plates supplemented with NIM, root growth was substantially inhibited by concentrations of NIM greater than 100 μM (Figure 7). Inhibition was even greater at equivalent concentrations of NA (Figure 7), consistent with the results reported by Zheng *et al.* (2005). When seedlings of wild-type plants and *nic1-1* mutants were first germinated on half-strength MS plates and then transferred to plates containing 0.2 mM NIM, the root growth of the *nic1-1* mutant plants was not inhibited but the root growth of the wild-type plants was (Figure 8). Moreover, transgenic *nic1-1* plants overexpressing a wild-type allele of *AtNIC1* had a much more severe phenotypic change compared with that of the wild-type plants. When seedlings were transferred to plates containing NA, the growth of the roots of both wild-type and mutant plants was inhibited (Figure 8). Furthermore, roots of wild-type plants growing on NIM and roots of both wild-type and *nic1-1* mutants growing on NA were twisted, and the epidermal cell files showed left-handed (S-form) helices when viewed under the microscope (Figure 8). While the complemented plants (35S:NIC1/*nic1-1*) did not show any difference from wild-type and *nic1-1* mutants when grown on half-strength MS plates containing 0.2 mM NA, their roots were inhibited much more heavily than wild-type and *nic1-1* mutants when grown on NIM, and their epidermal cell files were skewed much more strongly to the right than in the wild type and *nic1-1* mutants (Figure 8). In control experiments, wild-type, *nic1-1*, and 35S:NIC1/*nic1-1* plants were treated with 0.2 mM acetic acid, an acid with an almost identical p*K* to that of NA. This treatment did not inhibit root growth nor cause root twisting (data not shown).

The nic1-1 *mutant is hypersensitive to ABA and NaCl*

The ABA signal transduction pathway that plants employ to respond to conditions of stress such as drought and salinity requires NAD(P)H (Finkelstein *et al.*, 2002; Leon-Kloosterziel *et al.*, 1996). It has further been shown that the signal initiated by ABA causes the formation of cyclic ADP-ribose (cADPR), a compound derived from NAD (Wu *et al.*, 1997, 2003). Because of the reduced levels of NAD(H) and NADP(H) concentration in the *nic1-1* mutant compared with the wild type, we tested the response of the *nic1-1* mutant plants to treatment of exogenously added ABA and NaCl. When wild-type and *nic1-1* plants were germinated on half-strength MS plates supplemented with ABA, the growth of *nic1-1* seedlings was greatly inhibited compared with growth of the

Table 2 Concentrations of NAD(H) and NADP(H) in different organs of Col-0, *nic1-1* and AtNIC1-overexpressing plants

Tissue	Line	[NAD+] (nmol g^{-1} FW)	[NADH] (nmol g^{-1} FW)	Total NAD(H) (nmol g^{-1} FW)	[NAD+]/ [NADH]	[NADP+] (nmol g^{-1} FW)	[NADPH] (nmol g^{-1} FW)	Total NADP(H) (nmol g^{-1} FW)	[NADP+]/ [NADPH]
Root	Col-0	6.50 ± 0.56	0.20 ± 0.11	6.70 ± 0.74	31.4 ± 7.2	1.71 ± 0.80	0.30 ± 0.17	2.00 ± 0.39	5.65 ± 2.21
	nic1-1	3.29 ± 1.27	Trace	3.29 ± 0.64	–	1.21 ± 0.55	0.20 ± 0.11	1.41 ± 0.21	6.21 ± 1.56
	CHF2-4	12.0 ± 3.57	0.43 ± 0.25	12.4 ± 3.35	30.0 ± 5.6	1.99 ± 0.94	0.40 ± 0.23	2.39 ± 0.20	5.02 ± 1.25
	MDC8-5	12.4 ± 3.37	0.57 ± 0.33	13.0 ± 3.06	25.8 ± 6.1	1.66 ± 0.72	0.23 ± 0.14	1.88 ± 0.96	7.11 ± 2.87
Rosette leaves	Col-0	10.2 ± 2.84	4.48 ± 3.21	14.6 ± 5.72	2.81 ± 0.66	2.79 ± 0.65	Trace	2.79 ± 0.65	–
	nic1-1	5.84 ± 2.00	2.55 ± 1.80	8.39 ± 3.76	2.58 ± 0.45	1.43 ± 0.15	Trace	1.43 ± 0.15	–
	CHF2-4	15.2 ± 3.12	4.44 ± 1.87	19.5 ± 3.95	3.25 ± 0.70	3.11 ± 0.78	Trace	3.11 ± 0.78	–
	MDC8-5	14.8 ± 2.36	4.31 ± 1.96	18.4 ± 4.21	3.41 ± 0.83	2.95 ± 0.67	Trace	2.95 ± 0.67	–
Stem	Col-0	12.0 ± 4.25	Trace	12.0 ± 4.25	–	3.10 ± 0.28	Trace	3.10 ± 0.28	–
	nic1-1	3.94 ± 1.03	n.d.	3.94 ± 1.03	–	1.95 ± 0.38	Trace	1.95 ± 0.38	–
Cauline leaves	Col-0	11.3 ± 3.38	4.01 ± 2.71	15.3 ± 6.01	3.43 ± 0.79	3.58 ± 0.32	Trace	3.58 ± 0.32	–
	nic1-1	5.77 ± 2.74	2.28 ± 1.41	8.05 ± 3.88	3.33 ± 1.14	1.97 ± 0.29	Trace	1.97 ± 0.29	–
Flower	Col-0	27.0 ± 5.07	3.57 ± 3.03	30.6 ± 7.16	9.09 ± 3.13	4.50 ± 0.74	0.97 ± 0.34	5.47 ± 0.69	4.04 ± 1.20
	nic1-1	10.0 ± 1.89	1.97 ± 1.34	12.0 ± 2.84	8.79 ± 2.39	1.82 ± 0.29	0.34 ± 0.20	2.16 ± 0.48	3.64 ± 0.66
Silique	Col-0	17.9 ± 4.54	2.79 ± 1.28	20.7 ± 4.82	4.50 ± 1.42	3.77 ± 0.54	0.60 ± 0.10	4.37 ± 0.62	6.42 ± 0.53
	nic1-1	7.97 ± 2.10	1.57 ± 0.76	9.55 ± 2.53	4.93 ± 1.39	1.94 ± 0.51	0.45 ± 0.28	2.40 ± 0.78	5.73 ± 1.50
Seedlings	Col-0	9.9 ± 1.55	0.94 ± 0.24	10.8 ± 1.65	11.9 ± 2.31	2.02 ± 0.55	0.35 ± 0.11	2.37 ± 0.62	6.02 ± 1.73
	nic1-1	7.07 ± 0.37	0.38 ± 0.17	7.45 ± 0.43	13.5 ± 3.56	1.48 ± 0.23	0.33 ± 0.08	1.81 ± 0.27	4.98 ± 1.63
	CHF2-4	11.8 ± 1.41	1.23 ± 0.46	13.0 ± 1.72	9.49 ± 2.01	2.22 ± 0.37	0.42 ± 0.15	2.64 ± 0.46	5.43 ± 1.09
	MDC8-5	10.9 ± 1.70	1.03 ± 0.19	11.9 ± 1.74	11.3 ± 3.05	2.15 ± 0.31	0.39 ± 0.17	2.54 ± 0.40	5.68 ± 2.00

Data are presented as mean ± SD (*n* = 5).
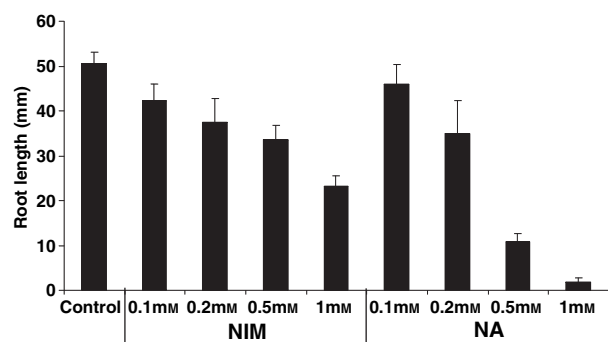n.d., not detected.

Figure 7. Inhibition of root growth of wild-type plants by NIM and NA. Seven-day-old Col-0 seedlings were grown on half-strength MS plates supplemented with different concentration of NIM and NA. Results are presented as the average root length of 12 seedlings for each point. Data are the mean ± SD of three independent experiments.

wild-type seedling (Figure 9a). The growth of *nic1-1* was also much more inhibited than wild-type plants when treated with 125 mM NaCl (Figure 9b).

We also measured and compared the content of NAD(H) and NADP(H) of 2-week-old seedlings under ABA and salt treatments. Under normal growth conditions, the total content of NAD(H) of *nic1-1* was only 70% of that found in the wild type (7.45 ± 0.43 nmol g^{-1} fresh weight (FW) vs.10.84 ± 1.65 nmol g^{-1} FW; Figure 9c). No significant differences were observed in the NAD(H) content of wild-type and NIC1-overexperssing transgenic plants (Figure 9c). Wild-type and overexpressor transgenic plants grown on half-strength MS medium supplemented with 1 μM ABA or 125 mM NaCl, showed a twofold increase in the content of total NAD(H) over the control; however, there was no increase in the total NAD(H) content in the *nic1-1* mutant under the same treatments (Figure 9c). For all plant lines, there were no significant changes in total NADP(H) or the NAD$^+$/NADH and NADP$^+$/NADPH ratios (data not shown).

Discussion

Synthesis of NAD consumes soluble, biologically available nitrogen that is scarce in natural environments and energetically expensive to produce. For this reason, all organ-

isms are known to have evolved an NAD salvage pathway that reuses NIM that was released from NAD at some point. Here we demonstrate that protein extracts of the various organs of wild-type, but not of *nic1-1* mutants, can convert NIM to NA. We also show that the concentrations of NAD(H) and NADP(H) in the major organs of wild-type plants are greater than the concentrations of these compounds in *nic1-1* plants. These observations indicate that in all major organs of Arabidopsis, NIM is first converted to NA by the action of AtNIC1, and NA is then incorporated into NAD(H) and NADP(H). Our results further show that AtNIC1, the protein encoded by *At2g22570*, is the enzyme responsible for most, if not all, of the conversion of NIM to NA in Arabidopsis under the growth conditions tested in this study. However, it appears that Arabidopsis also possesses at least one additional NIC enzyme, which is predominantly expressed in seeds (J. E. Gray, University of Sheffield, Sheffield, UK, personal communication).

Our results indicate that Arabidopsis has a similar NAD salvage pathway to that found in bacteria and yeast. In mammals, NIM is converted to NMN, but we could not detect labeled NMN when [^{14}C]-NIM was fed to Arabidopsis leaf disks (Figure 2). This result is consistent with the report of Zheng *et al.* (2005), who failed to detect any NPRTase activity in the cotyledon and embryonic axes of mungbean. Moreover, we could not find any NPRTase homologs in the Arabidopsis genome when blasted with a known NPRTase sequence from mouse (accession AAT72933; Revollo *et al.*, 2004). On the other hand, we clearly identified labeled NaMN, consistent with the observation of NaPRTase activity in coffee leaves and mungbean by Zheng *et al.* and the presence of NaPRTase homologs in the genome of Arabidopsis (Zheng and Ashihara, 2004; Zheng *et al.*, 2005).

The levels of NAD(H) and NADP(H) in different organs of *nic1-1* mutant plants were lower than those in the wild-type plants, and the differences were larger in organs of mature plants than in seedlings (Table 2 and Figure 9c). In yeast, the deletion in the *PNC1* gene, which encodes NIC, causes a threefold decrease in NAD$^+$ concentration in the stationary phase, but the concentration of intracellular NAD$^+$ was comparable in the exponential growth stage (Ghislain *et al.*, 2002). Our results suggest that NAD biosynthesis in Arabid-
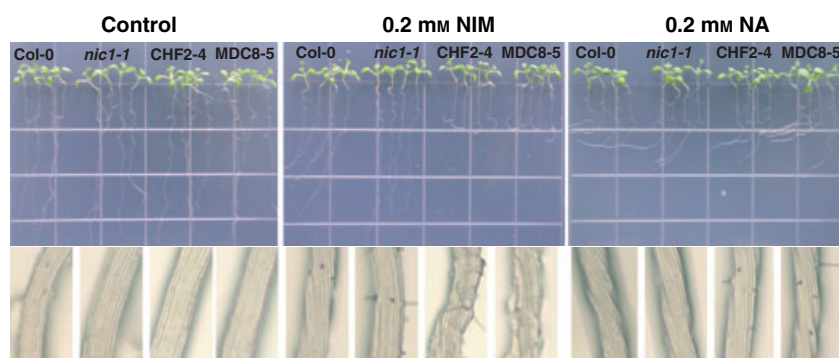

Figure 8. Root growth and morphology of wild-type, *nic1-1*, and NIC1-overexpressing plants exposed to NIM and NA.
Four-day-old seedlings were transferred from half-strength MS plates to plates supplemented with 0.2 mM NIM or 0.2 mM NA and grown for five additional days. Close-ups of root differentiated region are shown below. CHF2-4 and MDC8-5 are two lines of plants, described above (see Figure 5), which overexpress *AtNIC1* under the control of the 35S promoter in the *nic1-1* background.
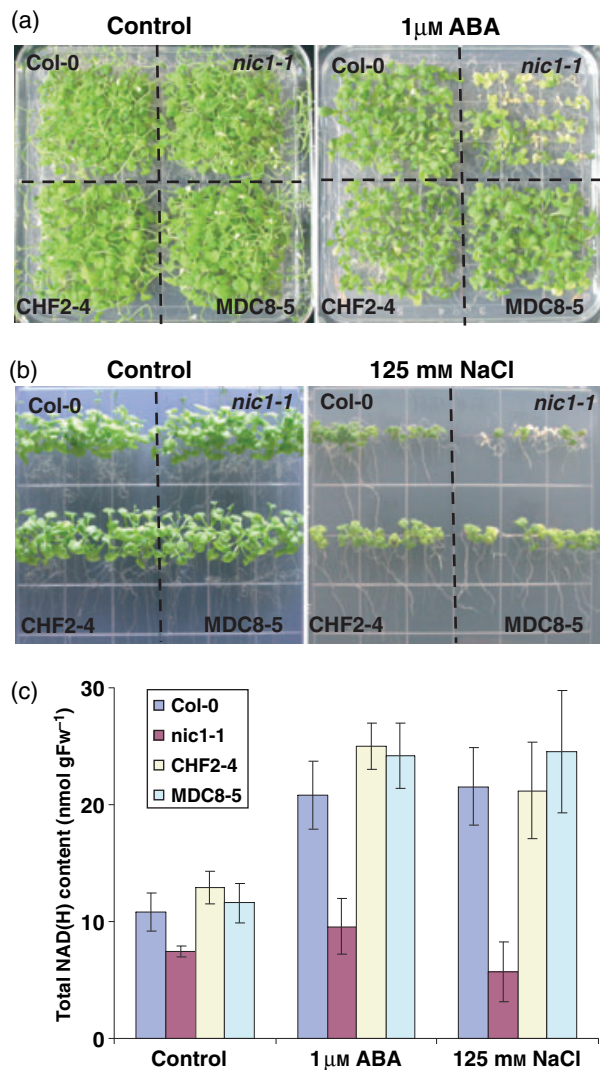
Figure 9. Inhibition of seedling growth in *nic1-1* mutant plants grown on ABA and NaCl.

(a) Three-week-old seedlings of Col-0, *nic1-1* and 35S:NIC1/*nic1-1* plants grown on half-strength MS plates with or without 1 μM ABA.

(b) Seedlings of Col-0, *nic1-1* and 35S:NIC1/*nic1-1* plants growing on half-strength MS plates with or without 125 mM NaCl.

(c) Quantitative measurements of total NAD(H) levels in seedlings grown under 1 μM ABA and 125 mM NaCl treatments. Data are presented as means ± SD of five independent experiments.

higher than those observed in stems and roots of the *nic1-1* mutant (although the relative decreases were of a more similar magnitude). A clear understanding of the relationship of NIC activity with actual levels of NAD(P)(H) in each organ will require a better understanding of the rate of turnover of these compounds.

Many physiological processes involved in the adaptation of plants to stresses such as draught and salinity are mediated in part by ABA through a signal transduction pathway that uses NAD(P)(H) to form cADPR (Wu *et al.*, 1997, 2003). Since it could be predicted that the *nic1-1* mutant plants would have lower levels of NAD(P)(H), we also predicted that their response to ABA and NaCl treatments would be impaired. Indeed, the mutant plants showed higher sensitivity to exogenously added ABA (1 μM concentration) and NaCl (125 mM concentration), exhibiting strong chlorosis and cessation of growth while wild-type plants were only mildly affected at the same concentrations of ABA and NaCl (Figure 9). Measurements showed that the wild-type plants (as well as the NIC1-overexpressing lines) responded to these treatments by increasing the amount of NAD(H) twofold, while in the *nic1-1* mutants the levels of NAD(H) did not change during these treatments compared with control treatment. While it is likely that both the *de novo* synthesis and the salvage pathway operate during ABA and NaCl treatments in wild-type plants, it appears that, because the mutant is not capable of recycling the degraded NAD(P), overall it is not capable of increasing the levels of these compounds in the cell.

The roots of wild-type seedlings treated with NIM and NA exhibited growth retardation, and the roots developed a twisted morphology (Figure 8). The cause of these effects is NA and not NIM, since the roots of *nic1-1* plants, which cannot convert NIM to NA, did not exhibit these phenotypes when grown on NIM, but do have growth inhibition and twisted morphology when grown on NA. Inhibition of root growth and twisted root morphology were also observed when plants were treated with the tubulin-specific drugs Taxol and propyzamide (Thitamadee *et al.*, 2002). It is therefore possible that the accumulation of NA disturbs the organization of microtubules.

Experimental procedures

Plant materials and RNA analysis

Arabidopsis thaliana (L.) Heynh (ecotype Col-0) plants, wild type and transgenic, were grown on soil in growth chamber set for 23°C and a 16-h light/8-h dark period. Total RNA isolation and RNA gel blot analysis were performed as prescribed by Chen *et al.* (2003).

Analysis of metabolism of [14C]-NIM in planta

Leaf disks (50 mg FW) were soaked in 1 ml of 10 μM [carboxyl-14C]-NIM solution for different periods (30 min, 2 h, 4 h and 24 h), after

opsis seedlings is due mainly to the *de novo* pathway from aspartate (Katoh *et al.*, 2006). Our results further indicate that in mature plants the NAD salvage pathway that recycles NIM back to NAD through NA contributes a larger portion to the NAD(P)(H) pool.

Interestingly, the organs with the highest concentrations of NAD(H), such as flower (30.6 ± 7.16 nmol g⁻¹ FW) and silique (20.7 ± 4.82 nmol g⁻¹ FW), exhibit three- to fourfold lower levels of NIC relative activity compared with stems and roots. Yet the actual decreases in NAD(P)(H) concentrations in flower and silique organs of *nic1-1* plants were

which the treated leaf disk were homogenized in a pestle and mortar with 250 µl of 20 mM sodium diethyldithiocarbamate. After centrifugation for 5 min at 22 000 *g*, 5 µl of supernatant was spotted on Polygram® TLC plates (Macherey-Nagel, http://www.macherey-nagel.com/) and developed with two developing solvent systems [ethyl acetate (EtOAC): acetic acid (HOAc; 100:1) and *n*-butanol:HOAc:H_2O (2:1:1)]. To identify radiolabeled metabolites, the chemical standards were spotted on the same plate. Radioactivity on the TLC plate was determined using an InstantImager radio scanner (Packard Instrument Company Inc., http://las.perkinelmer.com/).

Expression of AtNIC1 in E. coli *and purification*

A full-length *AtNIC1* cDNA clone was obtained from the Arabidopsis Biological Resource Center (stock number C105146) and confirmed by sequencing. The open reading frame of *AtNIC1* was amplified by PCR using the forward primer 5′-CACCATGGCGAATCATGAAACG-ATA-3′ and the reverse primer 5′-TCAAGTCTCAAAAGAAATTTTAG-3′. The resulting PCR fragment was cloned into pENTR®/D-TOPO vector (Invitrogen, http://www.invitrogen.com/) and subsequently transferred into pHis9GW vector (modified from pET-28 vector) for protein expression in *E. coli* by LR clonase reaction (Invitrogen). His-tagged AtNIC1 was obtained in BL21(+) cells and purified using Ni-NTA affinity columns as previously described (Tholl *et al.*, 2004). All PCR procedures were performed using *Pfu* DNA polymerase (Stratagene, http://www.stratagene.com/) to enhance fidelity. All constructs were verified by DNA sequencing.

Construction of the AtNIC1 promoter fusion to the β-glucuronidase (GUS) reporter gene and histochemical localization of GUS activity

An *AtNIC1* promoter fragment from 1974 to 4 bp upstream of the translation initiation codon was amplified from the genomic DNA of Col-0 by using the forward primer 5′-CACCTGAGATTAAGTTTA-GGTCGGTAAGATG-3′ and reverse primer 5′-GATACGAGTCTAG-AAAAAATTGAGAAAAC-3′. The resulting PCR fragment was cloned into pENTR®/D-TOPO vector and subsequently transferred into pMDC162GW binary vector (Curtis and Grossniklaus, 2003) by LR clonase reaction. Transformation of Arabidopsis, screening for homozygous transgenic plants and GUS staining were performed as described by Chen *et al.* (2003).

Enzymatic activity assays and product identification

To identify the product of enzyme reaction, the reaction was stopped by heating at 95°C for 5 min and followed by centrifugation for 5 min at 22 000 *g*, then 5 µl of the clear supernatant was injected into Symmetry® C18 column (15 cm × 2.1 mm internal diameter; Waters, http://www.waters.com/) attached to a 2690 HPLC (Waters) after. The mobile phase consisted of methanol–acetate buffer (pH 5) containing 0.1 M sodium acetate and 0.01 M tetrabutylammonium bromide (v.v, 15:85), and the flow rate was kept at 1 ml min^{-1} at room temperature. Compound elution was monitored at 200–400 nm with a Waters 996 UV/visible photodiode array detector.

For enzyme characterization experiments, appropriate concentrations of purified protein were incubated with different concentrations of NIM for 5 min at 30°C in a final volume of 100 µl containing a final concentration of 10 mM 2-amino-2-(hydroxymethyl)-1,3-propanediol (TRIS), pH 7.5, 150 mM NaCl and 1 mM $MgCl_2$. The concentration of the product, ammonia, was determined using the Sigma ammonia diagnostic kit (Sigma Chemical Co., http://www.sigmaaldrich.com/).

For enzymatic assays with [carboxyl-^{14}C]-NIM as substrate, 10 µM [carboxyl-^{14}C]-NIM was used for each reaction and incubated for 30 min at 30°C. Five microliters of enzyme reaction was spotted on a silica TLC and developed with EtOAC:HOAc (100:1) and compared with radiolabeled and non-labeled standards.

Isolation and complementation of the nic1-1 *T-DNA insertion mutant*

To verify the position of the insertion in the *AtNIC1* T-DNA insertion allele SALK_131410 (ecotype Col-0), the LBb1 primer (5′-GCGTGGACCGCTTGCTGCAACT-3′), annealing to the T-DNA left border, was first used together with the *AtNIC1*-specific primers mentioned above to amplify a fragment from genomic DNA. The amplified fragment was sequenced to determine the exact position of the T-DNA insertion. Plants homozygous for the *nic1-1* mutation were used for further analysis.

To exclude the interference of NPT II (kanamycin resistance gene) from T-DNA in *nic1-1* mutant plants, we selected two different vectors conferring the different antibiotic resistances of the transgenic plants (pCHF3GW has kanamycin resistance and pMDC32GW has hygromycin resistance) to make the complemented plants. The open reading frame of *AtNIC1* was transferred into the GATEWAY binary vectors from the pENTR vector following the manufacturer's instructions. In these vectors, the *AtNIC1* open reading frame was spliced downstream from the 35S promoter. The construct was transformed into *Agrobacterium tumefaciens* strain AGL1 and introduced into Arabidopsis plants via *A. tumefaciens*-mediated vacuum infiltration (Bechtold and Pelletier, 1998). Transgenic seeds were plated on half-strength MS medium containing 0.8% (w/v) agar, 2.3 g l^{-1} MS basal salt mixture and 50 µg ml^{-1} kanamycin (for transgenic seeds with the pCHF3GW construct) or 15 µg ml^{-1} hygromycin (for transgenic seeds with the pMDC32GW construct). The resistant seedlings were transplanted to soil and grown in the greenhouse to produce seeds. Homozygous complemented lines (*35S:NIC1/nic1-1*) were used for feeding experiments or stress treatments.

Measurement of NAD(H) and NADP(H) in wild-type and nic1-1 *mutant plants*

Measurements of NAD(P)H were performed as described by Hayashi *et al.* (2005). Briefly, 0.5 g plant tissue was grounded to fine powder in liquid nitrogen and divided equally into two parts. One aliquot was extracted with 0.5 ml 0.1 M HCl (for NAD$^+$ and NADP$^+$) and another aliquot was extracted with 0.5 ml 0.1 M NaOH (for NADH and NADPH) by heating at 95°C for 5 min. After cooling down in an ice bath, the pH was adjusted to 6.5 with NaOH (for acidic extract) or 7.5 with HCl (for basic extract). After the addition of 0.5 ml of 0.2 M glycylglycine to oxidized or reduced coenzyme fractions, respectively, the volume of each fraction was measured (around 1.4 ml). Each fraction was centrifuged (10 000 *g* for 20 min at 4°C), and the resulting supernatants were used for NAD(P)H measurement immediately. For NAD$^+$ and NADH measurements, 100 µl of extract were added to 500 µl of reaction mixture containing 50 mM glycylglycine (pH 7.4), 20 mM NIM, 1 mM phenazine methosulfate (PMS), 1 mM thiazolyl blue (MTT) and alcohol dehydrogenase (final concentration, 40 µg ml^{-1}). After placing the cuvette containing the reaction mixture in a UV/visible spectrophotometer for measurement at 570 nm, 50 µl of ethanol was added to start the reaction. For NADP$^+$ and NADPH measurements, 100 µl of extract was added to 500 µl of reaction mixture containing 50 mM glycylglycine (pH 7.4), 20 mM NIM, 1 mM PMS, 1 mM MTT and 2 mM glucose-6-phosphate. After placing the cuvette in a spectrophotometer for measurement

at 570 nm, glucose-6-phosphate dehydrogenase (final concentration, 1 μg ml^{-1}) was added to start the reaction. For the negative control, 100 μl of sterile water took the place of plant extract in the reaction. All those enzymatic cycling assays were performed in a dark-room and incubated at room temperature (22°C) for 5 min. The concentration of NAD(P)(H) in different extracts was determined by comparing sample values to a standard curve.

Acknowledgement

References

Alonso, J.M., Stepanova, A.V. and Leisse, T.J. (2003) Genome-wide insertional mutagenesis of *Arabidopsis thaliana*. *Science*, **301**, 653–657.

Ashihara, H., Stasolla, C., Yin, Y., Loukanina, N. and Thorpe, T.A. (2005) *De novo* and salvage biosynthetic pathways of pyridine nucleotides and nicotinic acid conjugates in cultured plant cells. *Plant Sci.* **169**, 107–114.

Bechtold, N. and Pelletier, G. (1998) *In planta* Agrobacterium-mediated transformation of adult *Arabidopsis thaliana* plants by vacuum infiltration. *Meth. Mol. Biol.* **82**, 259–266.

Berglund, T., Kalbin, G., Strid, A., Rydstrom, J. and Ohlsson, A.B. (1996) UV-B- and oxidative stress-induced increase in nicotinamide and trigonelline and inhibition of defensive metabolism induction by poly(ADP-ribose)polymerase inhibitor in plant tissue. *FEBS Lett.* **380**, 188–193.

Bieganowski, P. and Brenner, C. (2004) Discoveries of nicotinamide riboside as a nutrient and conserved NRK genes establish a Preiss-Handler independent route to NAD$^+$ in fungi and humans. *Cell*, **117**, 495–502.

Chen, F., D'Auria, J.C., Tholl, D., Ross, J.R., Gershenzon, J., Noel, J.P. and Pichersky, E. (2003) An *Arabidopsis thaliana* gene for methylsalicylate biosynthesis, identified by a biochemical genomics approach, has a role in defense. *Plant J.* **36**, 577–588.

Corpas, F.J., Barroso, J.B., Sandalio, L.M., Distefano, S., Palma, J.M., Lupianez, J.A. and Del Rio, L.A. (1998) A dehydrogenase-mediated recycling system of NADPH in plant peroxisomes. *Biochem. J.* **330**, 777–784.

Curtis, M.D. and Grossniklaus, U. (2003) A gateway cloning vector set for high-throughput functional analysis of genes in planta. *Plant Physiol.* **133**, 462–469.

Finkelstein, R.R., Gampala, S.S. and Rock, C.D. (2002) Abscisic acid signaling in seeds and seedlings. *Plant Cell*, **14**, S15–S45.

Ghislain, M., Talla, E. and Francois, J.M. (2002) Identification and functional analysis of the *Saccharomyces cerevisiae* nicotinamidase gene, *PNC1*. *Yeast*, **19**, 215–224.

Hayashi, M., Takahashi, H., Tamura, K., Huang, J., Yu, L.H., Kawai-Yamada, M., Tezuka, T. and Uchimiya, H. (2005) Enhanced dihydroflavonol-4-reductase activity and NAD homeostasis leading to cell death tolerance in transgenic rice. *Proc. Natl Acad. Sci. USA*, **102**, 7020–7025.

Hekimi, S. and Guarente, L. (2003) Genetics and the specificity of the aging process. *Science*, **299**, 1351–1354.

Hughes, D.E. and Williamson, D.H. (1953) The deamidation of nicotinamide by bacteria. *Biochem. J.* **55**, 851–856.

Hunt, L., Lerner, F. and Ziegler, M. (2004) NAD – new roles in signalling and gene regulation in plants. *New Phytol.*, **163**, 31–44.

Katoh, A. and Hashimoto, T. (2004) Molecular biology of pyridine nucleotide and nicotine biosynthesis. *Front. Biosci.* **9**, 1577–1586.

Katoh, A., Uenohara, K., Akita, M. and Hashimoto, T. (2006) Early steps in the biosynthesis of NAD in *Arabidopsis thaliana* start with aspartate and occur in the plastid. *Plant Physiol.* **141**, 851–857.

Kawai, S., Mori, S., Mukai, T., Hashimoto, W. and Murata, K. (2001) Molecular characterization of *Escherichia coli* NAD kinase. *Eur. J. Biochem.* **268**, 4359–4365.

Leon-Kloosterziel, K.M., van de Bunt, G.A., Zeevaart, J.A. and Koornneef, M. (1996) *Arabidopsis* mutants with a reduced seed dormancy. *Plant Physiol.* **110**, 233–240.

Lin, S.J., Defossez, P.A. and Guarente, L. (2000) Requirement of NAD and SIR2 for life-span extension by calorie restriction in *Saccharomyces cerevisiae*. *Science*, **289**, 2126–2128.

Outten, C.E. and Culotta, V.C. (2003) A novel NADH kinase is the mitochondrial source of NADPH in *Saccharomyces cerevisiae*. *EMBO J.* **22**, 2015–2024.

Raffaelli, N., Sorci, L., Amici, A., Emanuelli, M., Mazzola, F. and Magni, G. (2002) Identification of a novel human nicotinamide mononucleotide adenylyltransferase. *Biochem. Biophys. Res. Commun.* **297**, 835–840.

Revollo, J.R., Grimm, A.A. and Imai, S. (2004) The NAD biosynthesis pathway mediated by nicotinamide phosphoribosyltransferase regulates Sir2 activity in mammalian cells. *J. Biol. Chem.* **279**, 50754–50763.

Rongvaux, A., Andris, F., van Gool, F. and Leo, O. (2003) Reconstructing eukaryotic NAD metabolism. *Bioessays*, **25**, 683–690.

Schweiger, M., Hennig, K., Lerner, F., Niere, M., Hirsch-Kauffmann, M., Specht, T., Weise, C., Oei, S.L. and Ziegler, M. (2001) Characterization of recombinant human nicotinamide mononucleotide adenylyl transferase (NMNAT), a nuclear enzyme essential for NAD synthesis. *FEBS Lett.* **492**, 95–100.

Thitamadee, S., Tuchihara, K. and Hashimoto, T. (2002) Microtubule basis for left-handed helical growth in *Arabidopsis*. *Nature*, **417**, 193–196.

Tholl, D., Kish, C.M., Orlova, I., Sherman, D., Gershenzon, J., Pichersky, E. and Dudareva, N. (2004) Formation of monoterpenes in *Antirrhinum majus* and *Clarkia breweri* flowers involves heterodimeric geranyl diphosphate synthases. *Plant Cell*, **16**, 977–992.

Turner, W.L., Waller, J.C. and Snedden, W.A. (2005) Identification, molecular cloning and functional characterization of a novel NADH kinase from *Arabidopsis thaliana* (thale cress). *Biochem. J.* **385**, 217–223.

Wagner, R. and Wagner, K.G. (1985) The pyridine-nucleotide cycle in tobacco: enzyme activities for the *de novo* synthesis of NAD. *Planta*, **165**, 532–537.

Wagner, R., Feth, F. and Wagner, K.G. (1986) The pyridine-nucleotide cycle in tobacco: enzyme activities for the recycling of NAD. *Planta*, **167**, 226–232.

Wu, Y., Kuzma, J., Marechal, E., Graeff, R., Lee, H.C., Foster, R. and Chua, N.H. (1997) Abscisic acid signaling through cyclic ADP-ribose in plants. *Science*, **278**, 2126–2130.

Wu, Y., Sanchez, J.P., Lopez-Molina, L., Himmelbach, A., Grill, E. and Chua, N.H. (2003) The *abi1-1* mutation blocks ABA signaling downstream of cADPR action. *Plant J.* **34**, 307–315.

Zhang, X., Kurnasov, O.V., Karthikeyan, S., Grishin, N.V., Osterman, A.L. and Zhang, H. (2003) Structural characterization of a human cytosolic NMN/NaMN adenylyltransferase and implication in human NAD biosynthesis. *J. Biol. Chem.* **278**, 13503–13511.

Zheng, X.Q. and Ashihara, H. (2004) Distribution, biosynthesis and function of purine and pyridine alkaloids in *Coffea arabica* seedlings. *Plant Sci.*, **166**, 807–813.

Zheng, X.Q., Hayashibe, E. and Ashihara, H. (2005) Changes in trigonelline (*N*-methylnicotinic acid) content and nicotinic acid metabolism during germination of mungbean (*Phaseolus aureus*) seeds. *J. Exp. Bot.* **56**, 1615–1623.